

Analyst

Accepted Manuscript



This is an *Accepted Manuscript*, which has been through the Royal Society of Chemistry peer review process and has been accepted for publication.

Accepted Manuscripts are published online shortly after acceptance, before technical editing, formatting and proof reading. Using this free service, authors can make their results available to the community, in citable form, before we publish the edited article. We will replace this *Accepted Manuscript* with the edited and formatted *Advance Article* as soon as it is available.

You can find more information about *Accepted Manuscripts* in the [Information for Authors](#).

Please note that technical editing may introduce minor changes to the text and/or graphics, which may alter content. The journal's standard [Terms & Conditions](#) and the [Ethical guidelines](#) still apply. In no event shall the Royal Society of Chemistry be held responsible for any errors or omissions in this *Accepted Manuscript* or any consequences arising from the use of any information it contains.

Rapid Detection of Sugar Alcohol Precursors and Corresponding Nitrate Ester Explosives using Direct Analysis in Real Time Mass Spectrometry^{†‡}

Cite this: DOI: 10.1039/x0xx00000x

Edward Sisco^a and Thomas P. Forbes^a

Received 00th January 2012,
Accepted 00th January 2012

DOI: 10.1039/x0xx00000x

www.rsc.org/

This work highlights the rapid detection of nitrate ester explosives and their sugar alcohol precursors by direct analysis in real time mass spectrometry (DART-MS) using an off-axis geometry. Demonstration of the effect of various parameters, such as ion polarity and in-source collision induced dissociation (CID) on the detection of these compounds is presented. Sensitivity of sugar alcohols and nitrate ester explosives was found to be greatest in negative ion mode with sensitivities ranging from hundreds of picograms to hundreds of nanograms, depending on the characteristics of the particular molecule. Altering the in-source CID potential allowed for acquisition of characteristic molecular ion spectra as well as fragmentation spectra. Additional studies were completed to identify the role of different experimental parameters on the sensitivity for these compounds. Variables that were examined included the DART gas stream temperature, the presence of a related compound (i.e., the effect of a precursor on the detection of a nitrate ester explosive), incorporation of dopant species and the role of the analysis surface. It was determined that each variable affected the response and detection of both sugar alcohols and the corresponding nitrate ester explosives. From this work, a rapid and sensitive method for the detection of individual sugar alcohols and corresponding nitrate ester explosives, or mixtures of the two, has been developed, providing a useful tool in the real-world identification of homemade explosives.

Introduction

Rapid and sensitive detection of explosive devices and energetic materials, from initial synthesis and manufacture to post-detonation, continues to be of great interest to the fields of homeland security and forensic science. Traditionally, this area of research has focused on military-grade nitrated organic explosives such as nitroaromatics (i.e., trinitrotoluene, TNT), nitramines (i.e., cyclotrimethylene trinitramine, RDX), and nitrate esters (i.e., pentaerythritol tetranitrate, PETN).¹ Recently, there has been an increased interest in detection and source identification of homemade explosives (HMEs)^{2,3} which do not contain military-grade explosives, and instead are derived from more easily obtainable and commercially available ingredients. Two evolving classes of HMEs that are experiencing an increase in interest and research include nitrate esters and peroxide-based explosives.² This work focuses on nitrate ester explosives, which are synthesized via the nitration of alcohol groups from the respective sugar alcohol.⁴⁻⁶ Sugar alcohols, or polyols, are commonly branded as artificial or natural sweeteners, and are found in items such as chewing gum, sugar free candy, mouthwashes, vitamins, insecticides, and pharmaceuticals.⁷⁻¹⁰

The most widely studied nitrate ester explosive, pentaerythritol tetranitrate (PETN), is a major component of plastic explosives such as Semtex, Detasheet, and pentolite.¹¹⁻¹³ PETN has gained widespread use both militarily and commercially as a stable and insensitive explosive.¹⁴⁻¹⁶ Nitroglycerin (NG), another commercially available nitrate ester, is commonly found in smokeless gun powders and explosives such as dynamite.¹⁷ Ethylene glycol dinitrate (EGDN) is a less commonly used nitrate ester, that has been employed as an explosives vapor detection taggant due to its high volatility.¹⁸ Investigating potential detection techniques for these and other emerging nitrate esters is imperative as HMEs continue to evolve. Identification of precursor sugar alcohols is also important, as this information could lead to valuable forensic intelligence on the route of synthesis.

A number of different techniques have been utilized for the detection of explosive compounds and devices. Ion mobility spectrometry (IMS) is commonly used for trace explosives screening since it is rapid, sensitive, does not require extensive infrastructure, and can be easily field deployed.¹⁷⁻²² However, IMS does not provide the specificity offered by mass spectrometry (MS) based techniques. The forensic science

community commonly employs techniques such as gas chromatography mass spectrometry (GC/MS)^{23–27} or liquid chromatography mass spectrometry (LC/MS)^{28–31} for trace explosive detection and confirmation. While these techniques offer high specificity and sensitivity, their advantages come at the expense of lengthy sample preparation, long run times, and potential degradation of the compound of interest. A developing suite of techniques for explosives detection is the utilization of ambient ionization mass spectrometry (AI-MS).^{32,33} AI-MS offers a number of appealing characteristics relevant to both homeland security and forensic science. These techniques typically offer rapid (on the order of seconds) and sensitive analysis with high specificity, requiring little to no sample preparation. A number of AI-MS techniques have been shown to rapidly detect explosive compounds including desorption electrospray ionization (DESI),^{34–38} low temperature plasma (LTP),^{39–41} desorption electro-flow focusing ionization (DEFFI),^{42–44} direct atmospheric pressure photoionization (DAPPI),^{45–47} and direct analysis in real time (DART).^{24,48,49}

The present work examines the trace detection and mass spectral characteristics for a range of sugar alcohol precursors and nitrate ester explosives using DART-MS with off-axis geometry. The characteristic ionization and fragmentation pathways of nine sugar alcohols and four nitrate esters were investigated by DART-MS using a hydrodynamic-assist Vapur® interface coupled to an orthogonal time-of-flight (ToF) mass spectrometer. The polyols and explosives examined included ethylene glycol, glycerol, erythritol, pentaerythritol, xylitol, inositol, sorbitol, mannitol, maltitol, PETN, NG, EGDN, and erythritol tetranitrate (ETN). Due to the widely variable structural, physical, and chemical properties of these compounds, a range of different mass spectral characteristics and sensitivities were identified. A number of experimental variables were also evaluated, including DART gas stream temperature, incorporation of a dopant species, and the surface on which a sample was deposited. Mixtures of sugar alcohols and explosives were also examined in the context of the effect that varying concentrations of one compound had on the sensitivity of the other.

Experimental Methods

Materials

Liquid chromatography-mass spectrometry (LC-MS) Ultra Chromasolv® grade methanol was purchased from Sigma-Aldrich (St. Louis, MO). Sugar alcohols including: ethylene glycol, glycerol, erythritol, xylitol, sorbitol, mannitol, pentaerythritol, maltitol, and inositol were also purchased from Sigma-Aldrich at 98 percent purity or greater. Explosive standards: erythritol tetranitrate (ETN), pentaerythritol tetranitrate (PETN), nitroglycerin (NG), and ethylene glycol dinitrate (EGDN) were purchased from AccuStandard (New Haven, CT) at a concentration of 1 mg/mL, except EGDN at 0.1 mg/mL, in either methanol or acetonitrile. These materials

were deposited onto a number of different surfaces including: polytetrafluoroethylene (PTFE, Teflon) coated glass slides (Tekdon Inc., Mayakka City, FL), forensic lift tape (Sirchie Fingerprint Laboratories, Youngsville, NC), glass microscope slides (VWR, Radnor, PA), PTFE-coated fiberglass weave and Nomex swipe materials (DSA Detection, Boston, MA), and aluminum foil. Three dopant species were also used: methylene chloride, nitric acid, and acetone, all purchased from Sigma-Aldrich. Polyethylene glycol 400 (PEG 400) (Sigma-Aldrich) was used as the MS tuning compound, diluted in methanol.

Sample Preparation

Solutions of the sugar alcohols were prepared by dissolving the pure compounds in methanol to a concentration of approximately 1 mg/mL. These solutions, as well as the nitrate ester explosive solutions, were then serially diluted, in methanol, to desired concentrations ranging from 50 pg/μL to 100 ng/μL. Solution aliquots of 0.5 μL to 2 μL of each analyte were pipetted onto the surface of interest. For parametric studies and sensitivity measurements, the analytes were deposited onto the spots of the Teflon coated glass slides. For analysis from other surfaces, 100 ng of the sugar alcohols were deposited directly onto the surface of interest and analyzed.

Instrumentation

The technique evaluated in this work was direct analysis in real time mass spectrometry (DART-MS). Briefly, DART-MS is an ambient ionization technique that allows for sample introduction into the mass spectrometer through a two-step desorption-ionization process. The DART source itself consists of a needle electrode held at a potential of several kilovolts in a flowing stream of helium gas. The applied potential causes the formation of a plasma containing helium ions, electrons, and helium metastable atoms. Several grid electrodes downstream of the needle electrode are used to remove helium ions and electrons from the gas stream. After passing through the grid electrodes, the stream of helium metastable atoms is variably heated. Heating of the gas stream is required to facilitate thermal desorption of analyte molecules off of the sample surface. Subsequently, the sample is ionized through a series of Penning ionization reactions involving atmospheric gases and/or dopant molecules.⁵⁰ In-depth discussion of the hypothesized ionization mechanisms occurring in DART-MS are presented elsewhere.^{24,50,51}

A JEOL AccuTOF LC-plus JMS-T100LP time-of-flight mass spectrometer (JEOL USA, Peabody, MA) coupled with a Vapur® API interface (IonSense, Saugus, MA) was used for all experiments (Figure 1).[§] The Vapur® interface allowed for off-axis DART experiments, as the DART gas stream was directed into the mass spectrometer inlet via a mechanical roughing pump attached to the interface. A mass flow controller (Omega Engineering Inc., FMA 1842, Stamford, CT) monitored the inlet flow, approximately 3.8 L/min of N₂, at the interface at all times. Settings for the time-of-flight (ToF) mass spectrometer included a 100 °C orifice temperature, ±5 V ring lens voltage, ±10 V orifice 2 voltage, ±400 V peaks voltage, 40 *m/z* to 800

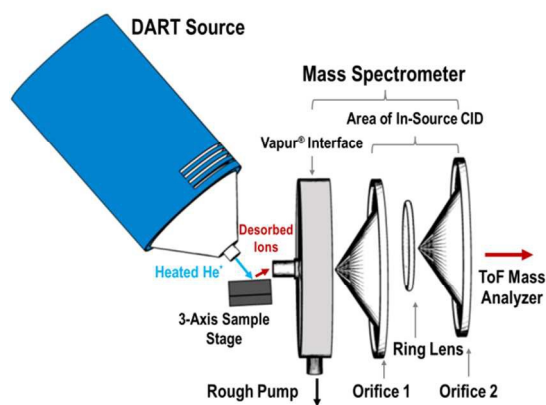


Figure 1. Schematic of the off-axis DART source geometry with the Vapur® API interface. Sample slides were placed on the 3-axis sample stage and interrogated with heated helium metastable atoms. The orifice 1 plate would typically be exposed to the atmosphere but in this setup was enclosed by the Vapur® interface. The potential difference between orifice 1 and orifice 2 controlled the extent of in-source CID.

m/z mass scan range at 0.5 s/scan, and ± 1950 V detector voltage. The ring lens and orifices controlled the ion trajectory into the mass spectrometer. In addition, the potential difference between orifice 1 – varied from ± 10 V to ± 90 V – and orifice 2 (Figure 1) determined the extent of in-source collision induced dissociation (CID). Generally, higher potential differences between the orifices led to increasing ion acceleration and more extensive fragmentation. The peak voltage corresponded to the voltage applied to the quadrupole in front of the ToF mass analyzer and correlated to the minimum mass that could be scanned.

A DART-SVP source (IonSense, Saugus, MA) was coupled to the ToF mass spectrometer. The source was mounted on a custom bracket, allowing for off-axis movement. Ultra-pure helium analysis gas was flowed at a rate of 1.5 L/min through a needle electrode with a -3000 V applied potential. Gas stream temperatures were varied from 150 °C to 400 °C. Samples were vertically mounted on a manual 3-axis stage (ThorLabs Inc., Newton, NJ) and positioned within 0.5 mm of the interface inlet to provide maximum signal intensity. The DART source was placed as close to the sample as possible within the geometrical constraints of the system (5 mm to 10 mm typically). The source angle of incidence relative to the sample was varied from 30 ° to 60 °. In all experiments, a particle vent and filter snorkel was placed near the DART inlet source to prevent release and inhalation of aerosols.

Results and Discussion

Traditionally, DART-MS analyses have been completed using on-axis transmission geometry. While this set-up allowed for optimal gas flow from the DART source to the mass spectrometer inlet, it made direct sampling of large surfaces (greater than several millimeters in width) difficult as large surfaces easily disrupted the gas flow and potentially blocked the MS inlet. Since direct analysis of an explosive residue

often involves larger surfaces (such as pieces of post blast materials or materials used in the synthesis of the explosive) a different means of sample analysis was necessary. Off-axis geometry, in which the sample was placed orthogonal to the MS inlet and interrogated by the DART source at an incidence angle between 0 ° (on-axis with the mass spectrometer inlet) and 90 ° (orthogonal to the mass spectrometer inlet) was required. This geometry was accomplished using the Vapur® interface, which pulled the gas stream towards the MS inlet. Since off-axis DART analysis has not been routinely studied, it was necessary to establish the angle of incidence that provided the greatest signal. Only angles ranging from 30 ° to 60 ° were examined, due to the large size and geometrical constraints of the DART source. To measure the effect of the incidence angle, 100 ng spots of xylitol were deposited and analyzed with four replicates. It was found that an optimal incidence angle was achieved at approximately 45 ° relative to MS inlet. A significant decrease in signal was observed as the angle was decreased to 30 ° (approximately one order of magnitude lower signal at 30 ° than at 45 °) while little change in signal was observed as the angle was increased towards 60 °. Since no additional benefit was noted past 45 °, and sampling became increasingly difficult past this angle due to geometrical constraints, 45 ° was used in all work.

Mass Spectral Characteristics of Sugar Alcohols and Nitrate Ester Explosives

A total of nine sugar alcohols were analyzed, as pure standards, in both positive and negative ionization modes to obtain characteristic spectra. The sugar alcohols analyzed included seven straight chain monosaccharides from two to six carbons in length, one ringed monosaccharide (inositol), and one disaccharide (maltitol). In all instances, mass spectra with peaks attributable to the sugar alcohol being analyzed were obtained regardless of ionization mode, as highlighted in Table 1. The representative spectra were obtained by interrogating 100 ng deposits using a 300 °C gas stream temperature without a dopant species. Characteristic peaks produced in both modes were found to be dependent on the potential difference between the two orifice plates of the time-of-flight (ToF) mass analyzer.

NEGATIVE ION MASS SPECTRA

In negative ionization mode, at an orifice plate voltage that minimized in-source collisional induced dissociation (CID) (-10 V), mass spectra of the sugar alcohols contained deprotonated molecular ions $[M-H]^-$ as well as adducts with molecular oxygen $[M+O_2]^-$, nitrite $[M+NO_2]^-$, and nitrate $[M+NO_3]^-$ (in all instances “M” refers to a sugar alcohol molecule). Oxygen, nitrite, and nitrate ions are commonly formed in DART analysis as helium metastable atoms ionize a number of atmospheric constituents.⁵⁰ Furthermore, in addition to monomer peaks, dimer peaks ($[2M-H]^-$, $[2M+O_2]^-$, $[2M+NO_2]^-$, and $[2M+NO_3]^-$) were typically detected for all of the above listed species. Figure 2(1A – 1C) and Tables 1 and 2 highlight these peaks in the representative spectra of erythritol, and other sugar alcohols, respectively, across varying first orifice plate

Table 1. Structures, average atomic masses, characteristic ion and structural assignments for all sugar alcohols examined.

Compound	a) MW ^a b) MP ^b c) VP ^c	Structure	Negative Ion Mass Spectra (-10 V Orifice 1)		Present at -30 V Orifice 1?	Positive Ion Mass Spectra (+10 V Orifice 1)		Present at +30 V Orifice 1?
			m/z	Ion		m/z	Ion	
Ethylene Glycol	a) 62.03678 b) -13 c) 8.11x10 ⁻³		61.02896 94.02661 123.06574 156.06339	[M-H] ⁻ [M+O ₂] ⁻ [2M-H] ⁻ [2M+O ₂] ⁻	Yes	80.07115 124.07356	[M+NH ₄] ⁺ [2M] ⁺	Yes
Glycerol	a) 92.04735 b) 20 c) 1.06x10 ⁻⁵		91.03952 124.03718 139.04025 183.08687 216.08452	[M-H] ⁻ [M+O ₂] ⁻ [M+NO ₂] ⁻ [2M-H] ⁻ [2M+O ₂] ⁻	Yes Yes	93.05517 110.08172 166.10793 149.08138	[M+H] ⁺ [M+NH ₄] ⁺ [M+NO] ⁺ [2M+HO ₂] ⁺	Yes Yes
Erythritol	a) 122.05791 b) 118 – 120 c) 6.99x10 ⁻⁸		121.05009 154.04774 168.05081 184.04573 243.10800 276.10565 290.10872 306.10364	[M-H] ⁻ [M+O ₂] ⁻ [M+NO ₂] ⁻ [M+NO ₃] ⁻ [2M-H] ⁻ [2M+O ₂] ⁻ [2M+NO ₂] ⁻ [2M+NO ₃] ⁻	Yes Yes Yes	123.06574 140.09228	[M+H] ⁺ [M+NH ₄] ⁺	Yes Yes
Pentaerythritol	a) 136.07356 b) 253 – 258 c) 3.37x10 ⁻⁹		135.06574 168.06339 182.06646 198.06138 271.13930 304.13695 318.1402 334.13494	[M-H] ⁻ [M+O ₂] ⁻ [M+NO ₂] ⁻ [M+NO ₃] ⁻ [2M-H] ⁻ [2M+O ₂] ⁻ [2M+NO ₂] ⁻ [2M+NO ₃] ⁻	Yes Yes Yes	137.08139 154.10793 290.18149	[M+H] ⁺ [M+NH ₄] ⁺ [2M+NH ₄] ⁺	Yes Yes
Xylitol	a) 152.06848 b) 94 – 97 c) 2.61x10 ⁻⁴		151.06065 184.05831 198.06138 214.05629 303.12913 336.12678 350.12988 366.12477	[M-H] ⁻ [M+O ₂] ⁻ [M+NO ₂] ⁻ [M+NO ₃] ⁻ [2M-H] ⁻ [2M+O ₂] ⁻ [2M+NO ₂] ⁻ [2M+NO ₃] ⁻	Yes Yes	153.07630 170.10285 322.17132	[M+H] ⁺ [M+NH ₄] ⁺ [2M+NH ₄] ⁺	Yes Yes
Inositol	a) 180.06339 b) 222 – 227 c) 1.77x10 ⁻¹¹		179.05557 212.05322 226.05629 242.05121 359.11896 392.11666	[M-H] ⁻ [M+O ₂] ⁻ [M+NO ₂] ⁻ [M+NO ₃] ⁻ [2M-H] ⁻ [2M+O ₂] ⁻	Yes Yes	198.09776	[M+NH ₄] ⁺	Yes
Sorbitol	a) 182.07904 b) 98 – 100 c) 1.75x10 ⁻¹⁰		181.07122 214.06887 228.07194 244.06686 363.15026 396.14791 410.15098 426.14590	[M-H] ⁻ [M+O ₂] ⁻ [M+NO ₂] ⁻ [M+NO ₃] ⁻ [2M-H] ⁻ [2M+O ₂] ⁻ [2M+NO ₂] ⁻ [2M+NO ₃] ⁻	Yes Yes	183.08687 200.11341 382.19245	[M+H] ⁺ [M+NH ₄] ⁺ [2M+NH ₄] ⁺	Yes Yes
Mannitol	a) 182.07904 b) 167 – 170 c) 1.75x10 ⁻¹⁰		181.07122 214.06887 228.07194 244.06686 363.15026 396.14791 410.15098 426.14590	[M-H] ⁻ [M+O ₂] ⁻ [M+NO ₂] ⁻ [M+NO ₃] ⁻ [2M-H] ⁻ [2M+O ₂] ⁻ [2M+NO ₂] ⁻ [2M+NO ₃] ⁻	Yes Yes	183.08687 200.11341 382.19245	[M+H] ⁺ [M+NH ₄] ⁺ [2M+NH ₄] ⁺	Yes Yes
Maltitol	a) 344.13187 b) 149 – 152 c) 2.98x10 ⁻¹⁸		161.04500 179.05557 181.07122	[C ₆ H ₉ O ₅] ⁻ [C ₆ H ₁₁ O ₆] ⁻ [C ₆ H ₁₃ O ₆] ⁻	Yes Yes Yes	180.08719 198.09776	[C ₆ H ₁₄ O ₅ N] ⁺ [C ₆ H ₁₆ O ₆ N] ⁺	Yes Yes

^aIn all cases the average atomic mass (“MW”, Da) was calculated using the MassCenterMain software, native to the AccuTOF system. ^bMelting points (“MP”, °C) of the respective compounds were obtained from the chemical manufacturers. ^cVapor pressures (“VP”, kPa at 25 °C) were estimated using “EPI Suite v4.11”. [US EPA. [2014]. Estimation Programs Interface Suite™ for Microsoft® Windows, v 4.11].

Table 2. Structures, average atomic masses, characteristic ion and structural assignments for all nitrate ester explosives examined.

Compound	a) MW ^a b) MP ^b c) VP ^c	Structure	Negative Ion Mass Spectra (-10 V Orifice 1)		Present at -30 V Orifice 1?	Positive Ion Mass Spectra (+10 V Orifice 1)		Present at +30 V Orifice 1?
			<i>m/z</i>	Ion		<i>m/z</i>	Ion	
Ethylene Glycol Dinitrate	a) 152.00694 b) -22 c) 5.19x10 ⁻¹		213.99475	[M+NO ₃] ⁻		N/A	N/A	N/A
Nitroglycerin	a) 227.00258 b) 14 c) 3.62x10 ⁻³		225.99475 272.99548 288.99040 303.99006	[M-H] ⁻ [M+NO ₂] ⁻ [M+NO ₃] ⁻ [M+HCO ₄] ⁻	Yes	N/A	N/A	N/A
Erythritol Tetranitrate	a) 301.99822 b) 61 c) 8.19x10 ⁻⁶		300.99040 347.99113 363.98604 378.98571 649.98935 665.98427	[M-H] ⁻ [M+NO ₂] ⁻ [M+NO ₃] ⁻ [M+HCO ₄] ⁻ [2M+NO ₂] ⁻ [2M+NO ₃] ⁻	Yes Yes Yes	N/A	N/A	N/A
Pentaerythritol Tetranitrate	a) 316.01387 b) 141 c) 5.61x10 ⁻⁷		315.00605 362.00678 378.00169 393.00136 678.02065 694.01557	[M-H] ⁻ [M+NO ₂] ⁻ [M+NO ₃] ⁻ [M+HCO ₄] ⁻ [2M+NO ₂] ⁻ [2M+NO ₃] ⁻	Yes Yes Yes	N/A	N/A	N/A

^aIn all cases the average atomic mass ("MW", Da) was calculated using the MassCenterMain software, native to the AccuTOF system. ^bMelting points ("MP", °C) of the respective compounds were obtained from the chemical manufacturers. ^cVapor pressures ("VP", kPa at 25 °C) were estimated using "EPI Suite v4.11". [US EPA. [2014]. Estimation Programs Interface Suite™ for Microsoft® Windows, v 4.11].

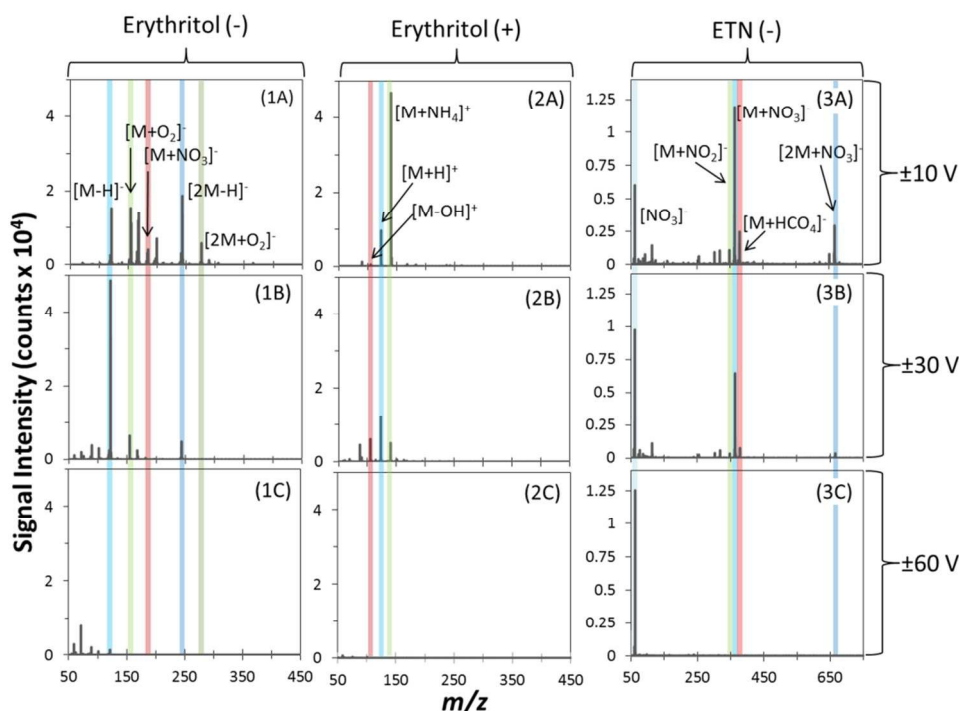


Figure 2 Representative mass spectra of erythritol in negative mode (1) and positive mode (2) as well as ETN in negative mode (3) at ±10 V (A), ±30 V (B), and ±60 V (C) orifice 1 plate voltages. Major peaks for each spectrum are highlighted.

voltages. Adduct and dimer formation occurred regardless of the size and structure of the sugar alcohol, with the exception of maltitol. Maltitol, the only disaccharide examined, consistently produced peaks corresponding to the cleavage of the bond at the oxygen joining the cyclic ring to the straight chain (Figure S1). Increasing the voltage applied to the first orifice plate from -10 V to -30 V caused dissociation of the majority of the

adduct species, simplifying the mass spectra to mainly the deprotonated molecular ion [M-H]⁻ and, in some instances, the deprotonated dimer species [2M-H]⁻ (Figure 2 (1B)). The reduction in adduct ions was accompanied by an increase in signal intensity of the deprotonated molecular ion by a factor of two or more. The increase in signal of the deprotonated molecular ion was likely due to fragmentation of adducted

species, via loss of the adduct ion and a proton within the inlet of the mass spectrometer. An increase in low mass fragments was also noted at -30 V and was mainly attributed to adduct species. Increasing the first orifice plate voltage past -30 V induced an increasing degree of fragmentation of the molecule. A -60 V first orifice plate voltage led to characteristic fragmentation across all sugar alcohols (Figure 2 (1C)). These fragment ions were largely similar amongst the sugar alcohols investigated. Common fragment ions included: $[C_2H_5O]^+$ (45 m/z), $[C_3H_7O]^+$ (59 m/z), and $[C_4H_9O_2]^+$ (89 m/z). When a -90 V potential was applied to the first orifice plate, almost complete fragmentation of the sugar alcohols was noted along with peak intensities nearing background noise. Little useful information could be obtained at this orifice plate voltage.

POSITIVE ION MASS SPECTRA

For sugar alcohols in positive ionization mode, at a +10 V first orifice plate voltage mass spectra were dominated by ammonium adduct monomers $[M+NH_4]^+$. Ammonia is another common atmospheric species ionized by DART. Protonated monomers $[M+H]^+$ and dimers $[2M+H]^+$ as well as ammonium adduct dimers $[2M+NH_4]^+$ were also commonly produced in these spectra (Figure 2 (2A) and Table 1).

Excluding maltitol and inositol, characteristic ion distributions were shifted toward the protonated molecular ion at +30 V orifice plate potential (Figure 2 (2B)). Inositol continued to preferentially form the ammonium adduct at +30 V (Figure S3) while maltitol exhibited fragmentation similar to that seen in negative mode (Figure S1). At +60 V (Figure 2 (2C)) and +90 V first orifice plate voltages, the sugar alcohols were heavily fragmented into a largely identical set of ions including: $[C_3H_7O]^+$ (59 m/z), $[C_4H_7O]^+$ (71 m/z), and $[C_5H_9O]^+$ (85 m/z). In both positive and negative mode, the differentiation of the two isomeric sugar alcohols, sorbitol and mannitol, was not possible due to identical adduct formation and fragmentation.

Low Level Detection of Sugar Alcohols and Corresponding Explosives

The DART-MS performance for detection of both the nitrate ester explosives and their sugar alcohol precursors was quantified by sensitivity measurements. Sensitivity of the technique for neat samples, which was determined in negative mode for all compounds studied and in positive mode for sugar alcohols, was defined as the lowest mass of deposited analyte measured resulting in an analyte-specific base peak distinguishable from background with a signal-to-noise (S/N) ratio of at least 3:1 above background. Four replicate measurements for each sugar alcohol were conducted and the lowest detectable masses (at or above 3:1 S/N) and average signal-to-noise ratios are depicted in Figure 3. In all instances, detection of the sugar alcohol precursor was possible at a lower mass than the nitrate ester explosive (data not shown). Figure 3 highlights three distinct ranges of sensitivities: sub-nanogram, single nanograms, and tens to hundreds of nanograms. When the structures of these chemicals that fall into these three

categories were analyzed, it was noted that that the least sensitive compounds were those with the highest and lowest volatilities within the components analyzed. As a tangible and quantified material property, volatility was used to describe the differences likely due to variability in bond energies between molecules. For compounds with the highest and lowest volatilities (or low and high binding energy), desorption was either too rapid (for high volatility compounds) or too slow (for low volatility compounds) to obtain sensitivities consistent with mid-range volatility samples. For molecules desorbed too rapidly, the instrument parameters (scan rate, etc.) limited the compounds detection. Alternatively, for molecules with very low volatilities, only a fraction of the deposited compound was desorbed and detected during the experiment duration. The sub-nanogram cluster of sugar alcohols, containing compounds used to optimize the method corresponded to those with the middle range of volatilities (and therefore binding energies). Enhanced detection of the low and high volatility compounds may be possible with changes in the DART sampling parameters, namely gas stream temperature.

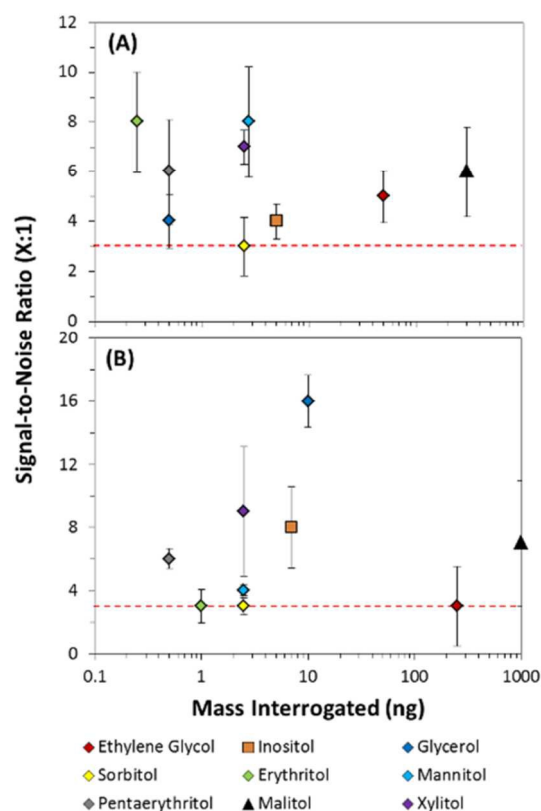


Figure 3 Measured sensitivities and average signal-to-noise ratios (S/N) for sugar alcohols in both negative (A) and positive (B) ionization mode. Error bars represent the standard deviation in the S/N measurement across 4 measurements. The dotted red line indicates the threshold of 3:1 S/N.

For sugar alcohols, detection was possible at lower mass in negative ionization mode than in positive ionization mode. Also, detection of sugar alcohols was more sensitive than detection of nitrate ester explosives. Higher sensitivity for the sugar alcohols may be related to the different ionization

pathways favored by sugar alcohols versus nitrate ester explosives. For sugar alcohols, where one of the main characteristic ion formation mechanisms was deprotonation, an excess of hydroxide ions was likely present in the gas stream, allowing for proton removal and detection at low levels.⁵¹ Nitrate ester explosives, however, ionize predominantly through nitrate adduct formation, involving ions from atmosphere as well as from fragmentation of the explosives. Detection of these compounds at the levels of the sugar alcohols might have been hindered by an insufficient number of explosive molecules left after fragmentation to be detected by DART source or by the several orders of magnitude difference in vapor pressures. The response of these compounds was found to be linear in the range of single nanograms to one hundred nanograms (Figure S4).

Analysis of Sugar Alcohol and Nitrate Ester Explosive Mixtures

Since real world HMEs could contain mixtures of sugar alcohol precursors and explosives, simultaneous detection of both the nitrate ester explosive and its sugar alcohol precursor (i.e. erythritol and ETN) were attempted. To identify if simultaneous detection was possible, and to what extent the sensitivity was hindered by the presence of the respective corresponding molecule, two pairs, ETN / erythritol and PETN / pentaerythritol were analyzed and the S/N ratio of each compound, at the lowest measurable concentration, in the presence of 0 ng, 1 ng, 10 ng, 100 ng, and 1,000 ng of its corresponding precursor/explosive molecule was determined (Figure 4 & Figure S5). The S/N measurements across this range again highlighted different ionization pathways for the sugar alcohols and nitrate esters. In the case of both ETN and PETN, sensitivity was maintained in the presence of any amount of sugar alcohol precursor, as there was little to no change to the S/N ratio.⁵² The reason for the consistent sensitivity was likely two-fold. First, the nitrate adduct formation pathway of the sugar alcohol may not lower the available atmospheric nitrate for the explosive molecules to adduct with, as the explosives have a higher affinity for free nitrate ions than sugar alcohols.⁵³ Second, fragmentation of the nitrate ester explosive may provide additional nitrate ions, regardless of the concentration of nitrate ions in the surrounding atmosphere. Conversely, the presence of even a small amount (10 ng) of nitrate ester explosive hindered the sensitivity for the corresponding sugar alcohol. As the amount of nitrate ester was increased, sensitivity for the sugar alcohols was further decreased, as evidenced by the decrease in S/N ratio, (Figure 4). In the presence of 1,000 ng of the nitrate ester explosive, the S/N ratio of the 25 ng deposits of erythritol and pentaerythritol roughly matched the S/N ratio of 0.25 ng to 0.50 ng deposits when analyzed without the presence of the nitrate ester, corresponding to up to a factor of 200 decrease in sensitivity for these two sugar alcohols. This reduction in sugar alcohol sensitivity could be due to either a change in the gas phase chemistry because of the presence of the nitrate ester (i.e., a change in acidity that affects the ability for deprotonation to occur) or because of a potentially higher

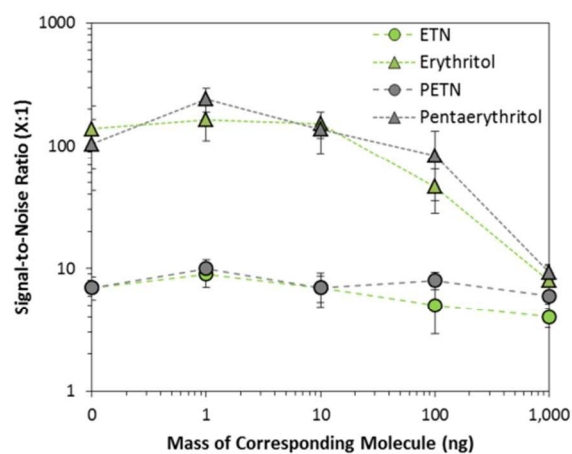


Figure 4 Average signal-to-noise (S/N) ratios of sugar alcohols and nitrate ester explosives in the presence of varying levels of the corresponding molecule. The corresponding molecule was either the sugar alcohol (e.g. erythritol was the corresponding molecule for ETN) or nitrate ester explosive (i.e., PETN was the corresponding molecule for pentaerythritol). Error bars represent the standard deviation of four replicate measurements.

affinity of the nitrate ester explosives to react with atmospheric species responsible for sugar alcohol deprotonation. Future work will focus on identifying which process was responsible for lowering the sensitivity of the sugar alcohols and what methods can be implemented to mitigate the impact. It is important to note that in most circumstances the goal of the analysis would be to identify the explosive compound. Since the explosives were shown to be unaffected by the presence of the sugar alcohol, detection in a real world mixture should not be hindered by the presence of a large excess of sugar alcohol precursors.

Effect of DART Gas Stream Temperature on Response

As demonstrated above, the sugar alcohols and nitrate ester explosives investigated spanned a wide range of melting points and vapor pressures. Several experimental variables were investigated to establish their effect on detection and sensitivity. One of the variables investigated was DART gas stream temperature – a crucial variable for analyte desorption.⁵⁰ While sufficient impinging gas temperature is necessary to thermally desorb the sample, an excessive gas stream temperature may lead to thermal degradation of the sample, especially in compounds prone to fragmentation such as EGDN. High gas stream temperatures may also lead to a high rate of desorption that results in ionization of only a small fraction of the neutral desorbed molecules. This phenomenon would be especially pronounced with high volatility compounds, where there may be inadequate time for rejuvenation of ionizing species. Here, 100 ng deposits of four different sugar alcohols and three explosives were interrogated by DART gas stream temperatures ranging from 150 °C to 400 °C. Four replicates were completed for each compound at each temperature. The four selected sugar alcohols reflected a range of melting points (MP) and vapor pressures (VP), as well as both straight chained and

ringed structures and included: glycerol, xylitol, pentaerythritol, and inositol. PETN, ETN, and NG were the three explosive molecules examined. Figure 5 displays the response of these compounds as a function of increasing gas stream temperature. The straight chained sugar alcohols were readily detected across the range of gas stream temperatures (Figure 5A), with

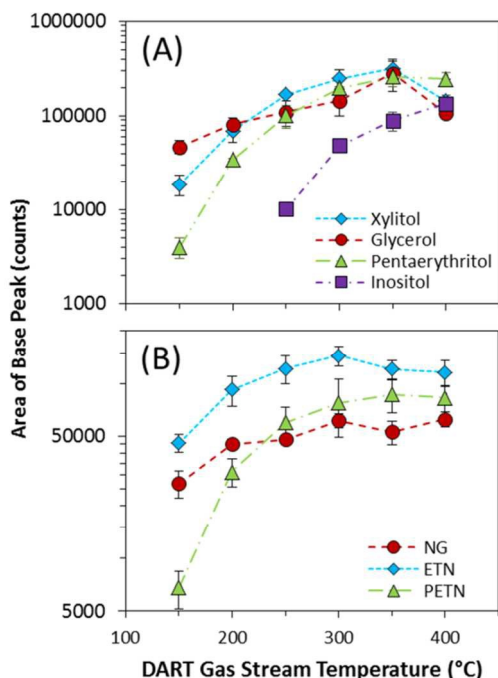


Figure 5 Effect of DART gas stream temperature on select sugar alcohols (A) and nitrate ester explosives (B). In both instances the data points represent the average peak area obtained by integrating the total area under the extracted ion chromatogram of the base peak ($[M-H]^-$ for sugar alcohols and $[M+NO_3]^-$ for nitrate ester explosives). Uncertainty is expressed as the standard deviation of four replicate samples.

maximum signal intensity observed at 350 °C, regardless of MP or VP. Conversely, the ring structured sugar alcohol, inositol, was undetectable at temperatures below 250 °C but demonstrated increasing response with temperatures above 250 °C. The difference in temperature responses between the straight chain and ringed sugar alcohols was likely due to differences in VP between the two classes. The estimated VP of the ringed structure was two to seven orders of magnitude lower than the straight chained sugar alcohols, and therefore VP may have significantly impacted the thermal desorption efficiency at lower gas stream temperatures.

The three explosives demonstrated similar trends to their corresponding sugar alcohol precursors as a function of gas stream temperature (Figure 5B). Optimal signal for all three compounds was achieved at 300 °C, with a slight decrease in signal noted beyond 300 °C for NG and ETN. The slightly lower optimal temperature of the nitrate ester explosives relative to the sugar alcohols is also believed to correspond to differences in VP. The explosive compounds have estimated VPs one to three orders of magnitude higher than their corresponding sugar alcohol precursors. Higher VPs allowed

for a rapid desorption of the explosives at lower gas stream temperatures.

Addition of Dopant Species

In addition to optimizing analyte desorption through temperature variation based on the physical and chemical properties of the compound(s) of interest, DART-MS sensitivity may be enhanced through optimized ionization. Incorporation of a dopant into the sampling region is one potential route for enhancing ionization by DART. Dopant and reactive species have demonstrated signal enhancement through two different mechanisms; either by providing a species for molecules to adduct with or by altering the chemical properties of the gas phase near the sampling region to emphasize certain ionization pathways.⁵⁰ Here, the efficacy of three dopant species, nitric acid (HNO_3), methylene chloride (CH_2Cl_2), and acetone (C_3H_6O), incorporated into the sampling scheme were evaluated. Nitric acid and methylene chloride readily form anions (NO_3^- and Cl^- , respectively) that have been shown to effectively adduct with various analytes, including nitrate ester explosives.⁵⁰ Alternatively, acetone does not typically form adduct species, but instead aids in the enhancement of molecular deprotonation through reduction of gas phase acidity in the sampling region.⁵¹ Incorporation of the dopant species into the sampling region was completed via one of two methods. Nitric acid, due to its lower volatility, was pipetted (1 μL of a 0.025 % by volume solution in methanol) directly onto the Teflon spot for simultaneous interrogation with the respective analyte. The higher volatility compounds, acetone and methylene chloride, were added by leaving a small open container near the DART source (approximately 5 cm away) during analysis. Dopants were evaluated, with appropriate ventilation, by interrogating 100 ng deposits of four sugar alcohols (xylitol, glycerol, pentaerythritol, and inositol) and three explosives (NG, ETN, and PETN), both neat and in the presence of each dopant.

The difference in the dominant ionization pathway of the two classes of compounds was highlighted by their response in the presence of certain dopants (Figure 6). For sugar alcohols, where deprotonation was observed as the major ionization pathway, the presence of additional adduct forming species (nitric acid and methylene chloride) decreased the signal of the base peak, as the opportunities for adduct formation increased (Figure 6A and Figure S6). Alternatively, the introduction of acetone enhanced the deprotonated molecular ion response for sugar alcohols. The presence of nitric acid did increase the nitrate adduct signal (Figure S6 and Figure S7), however, it did not enhance it significantly enough to surpass the deprotonated molecular ion signal as the base peak. Nitrate ester explosives (Figure 6B), which exhibited adduct formation with free nitrate ions as the major ionization pathway, showed the greatest improvement in signal with the addition of nitric acid. The response of ETN and PETN was increased by at least a factor of two because of the incorporation of nitric acid. The response of ETN and PETN was increased by at least a factor of two because of the incorporation of nitric acid, and proved to be

statistically different, when compared to the no dopant case (Student's t-test with a p-value of ≤ 0.05). The other adduct forming species, methylene chloride, did not improve the response of the explosive compounds, as the atmospheric nitrate ions appeared to be favored over the chloride ion. Regardless of the dopant used, the base peak remained the deprotonated molecular ion for the sugar alcohol and nitrate ion adduct for the sugar alcohols and nitrate ester explosives, respectively.

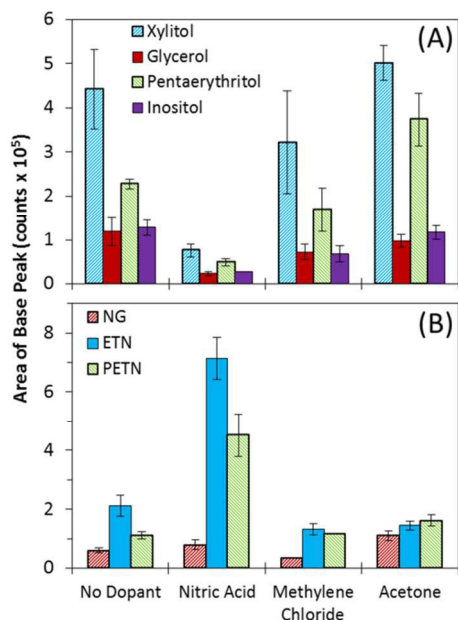


Figure 6 Response of representative sugar alcohols (A) and nitrate ester explosives (B) in the presence of select dopants. The peak area represents the area of the base peak ([M-H]⁻ for sugar alcohols and [M+NO₃]⁻ for nitrate ester explosives) from the extracted ion chromatogram. Uncertainty is expressed as the standard deviation of four replicate samples.

Incorporation of a dopant species may enhance the sensitivity of the technique or be used to selectively ionize one compound type over another. A separate experiment was completed where three of the nitrate ester explosives were run at the lowest detectable levels at or above 3:1 S/N in the presence of nitric acid and the signal-to-noise ratios were measured. The S/N of the base peaks increased from 7:1 to 215:1 for ETN, 7:1 to 123:1 for PETN, and 7:1 to 8:1 for NG. Sensitivity increases were greater for ETN and PETN because these species had lower volatilities than nitric acid. This allowed for desorption and ionization of the nitric acid prior to desorption of ETN or PETN. NG, however, was more volatile than nitric acid and therefore likely desorbed off of the surface prior to bulk desorption of nitric acid, minimizing the advantageous effects of free nitrate ions.

Detection off of Different Surface

In the previous sections, the main components of ambient ionization – desorption and ionization – were investigated and characterized for DART-MS detection, focusing on the analyte properties. Other aspects that could affect the response of a

sample are the physical and chemical properties of the substrate surface. In real-world situations, analyses would need to be completed off of a wide range of different surfaces. To evaluate the efficacy of the technique for detection of compounds off of realistic surfaces, five additional surfaces were evaluated. Since it was believed that the role of the surface would outweigh whether a sugar alcohol or nitrate ester explosive was deposited, only sugar alcohols were evaluated. Three characteristic sugar alcohols – xylitol, pentaerythritol, and inositol – were deposited in 100 ng spots onto five surfaces; glass (in the form of a glass microscope slide), common swipe materials: a PTFE-coated fiberglass weave and Nomex (a meta-aramid polymer), adhesive tape, and aluminum foil. Detection from all surfaces was demonstrated for each of the three sugar alcohols tested (Figures 7 and S8). The results established a number of surface topography and material property effects that directly contributed to enhancing or limiting analyte detection. Considering the Teflon spots as the reference case, materials that resulted in reduced local analyte surface concentrations led to poorer response. For example, the low surface tension between the deposited solvent and glass surface led to significant wetting and an overall large surface area distribution. Similarly, the Nomex fiber polymer swab (approximately 20 μm diameter fibers) readily wicked the liquid deposited sugar alcohols, again resulting in larger surface coverage and lower surface concentration relative to the Teflon substrate. The high thermal conductivity of the metallic

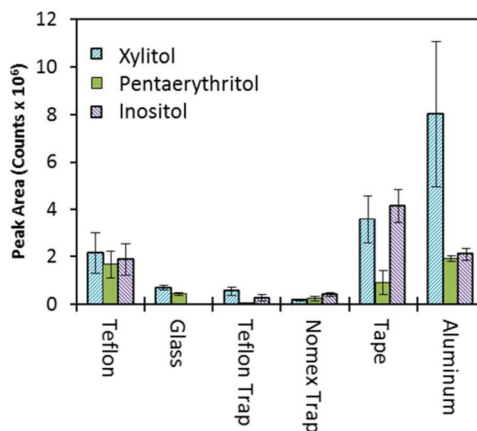


Figure 7 Effect of different surfaces on the detection of xylitol (blue), pentaerythritol (green), and inositol (purple). In all cases, four 100 ng deposits were analyzed and the total peak area of the base peak ([M-H]⁻) in the extracted ion chromatograms was calculated. Uncertainty is expressed as the standard deviation of four replicate samples.

aluminum surface exhibited signal enhancement for select sugar alcohols, specifically xylitol. The heated DART gas stream led to thermal desorption through direct contact and secondary substrate heating. Pentaerythritol and inositol did not demonstrate comparable increases in signal intensity from aluminum, likely due to their significantly higher melting points. Signal suppression due to surface topography was also observed. The relatively large weave structure/topography of

the PTFE-coated fiberglass swabs (interlacing 500 μm threads) led to disruptions in the impinging DART helium gas flow as well as reduced desorption from analyte recessed in the weave structure. In addition to material and topographical surface properties, the chemical composition of a substrate may impact detection. The adhesive components of the forensic lift tape investigated did not noticeably interfere with the detection of these sugar alcohols (Figure S8).

Conclusions

Detection of nitrate ester explosives and their sugar alcohol precursors was demonstrated with DART-MS. The Vapur[®] interface enabled off-axis analysis of these compounds deposited onto a number of different surfaces. Analysis surface appeared to play a critical role in signal response where non-uniform and wicking surfaces decreased signal response due to gas stream disruptions and larger sampling areas, respectively. Altering the in-source CID allowed for both characteristic molecular ion and fragmentation spectra to be obtained. This type of dual-spectra may allow DART-MS to give conformational information on the presence of sugar alcohols and/or nitrate ester explosives, as has been shown with narcotics analysis.⁴⁹ While changing the DART gas stream temperature did affect signal response of both classes of compounds, the more promising variable for increasing sensitivity and, potentially selectivity, was dopant incorporation. Addition of nitric acid to the sample was shown to drastically increase the response of the less volatile nitrate ester explosives, providing up to a 30-fold increase in signal-to-noise at low levels. Addition of adducting species has been shown to boost the signal of nitrate ester explosives with other ambient ionization techniques as well.^{24,34} If the identification of the sugar alcohol precursor is necessary, incorporation of acetone was shown to increase signal intensity, mimicking results of other studies⁵¹ and again highlighting acetone's role in emphasizing deprotonation pathways. In real-world sampling it is possible that homemade nitrate ester explosives will be contaminated with the sugar alcohol precursors. The presence of such an impurity did little to affect the DART-MS sensitivity for the explosive compounds, even when the sugar alcohol was present at several orders of magnitude higher concentrations than the explosive. This supports the rapid detection of compounds in real world settings by DART-MS. Off-axis DART-MS demonstrated rapid and sensitive detection of both sugar alcohols and nitrate ester explosives. Future work will aim to identify and characterize the mechanisms by which the sensitivity of sugar alcohols was decreased in the presence of nitrate esters. In conjunction, the role of competitive ionization and relative affinities of corresponding molecules both as pure mixtures and in the presence of dopants and impurities will be explored.

Acknowledgements

The U.S. Department of Homeland Security Science and Technology Directorate sponsored a portion of the production

of this material under Interagency Agreement IAA HSHQDC-12-X-00024 with the National Institute of Standards and Technology (NIST).

Notes and references

^a National Institute of Standards and Technology, Materials Measurement Science Division, Gaithersburg, Maryland 20899, United States. E-mail: edward.sisco@nist.gov

† Electronic Supplementary Information (ESI) available: Additional experimental details, spectra, and figures. See DOI: 10.1039/c000000x/

‡ Official contribution of the National Institute of Standards and Technology; not subject to copyright in the United States.

§ Certain commercial products are identified in order to adequately specify the procedure; this does not imply endorsement or recommendation by National Institute of Standards and Technology, nor does it imply that such products are necessarily the best available for the purpose.

- 1 J. Yinon, *Counterterrorist Detection Techniques of Explosives*, Elsevier, 2011.
- 2 D. Menning and H. Östmark, in *Detection of Liquid Explosives and Flammable Agents in Connection with Terrorism*, eds. H. Schubert and A. Kuznetsov, Springer Netherlands, 2008, pp. 55–70.
- 3 C. K. Hilton, C. A. Krueger, A. J. Midey, M. Osgood, J. Wu and C. Wu, *Int. J. Mass Spectrom.*, 2010, **298**, 64–71.
- 4 R. Boschan, R. T. Merrow and R. W. van Dolah, *Chem. Rev.*, 1955, **55**, 485–510.
- 5 R. Schulte-Ladbeck, P. Kolla and U. Karst, *Anal. Chem.*, 2003, **75**, 731–735.
- 6 J. P. Agrawal, R. N. Surve, Mehilal and S. H. Sonawane, *J. Hazard. Mater.*, 2000, **77**, 11–31.
- 7 R. C. Deis, *Cereal Foods World*, 2000, **45**, 418–421.
- 8 P. Tomasik, *Chemical and Functional Properties of Food Saccharides*, CRC Press, 2003.
- 9 W. S. Fedor, J. Millar and A. J. Accola, *Ind. Eng. Chem.*, 1960, **52**, 282–286.
- 10 P. Tundo, A. Perosa and F. Zecchini, Eds., in *Methods and Reagents for Green Chemistry*, John Wiley & Sons, Inc., 2007, pp. i–xvii.
- 11 J. Akhavan, *Spectrochim. Acta Part Mol. Spectrosc.*, 1991, **47**, 1247–1250.
- 12 J. R. Hobbs, in *Advances in Analysis and Detection of Explosives*, ed. J. Yinon, Springer Netherlands, 1993, pp. 409–427.
- 13 B. W. Asay, J. B. Ramsay, M. U. Anderson and R. A. Graham, *Shock Waves*, 1994, **3**, 267–271.
- 14 J. Yinon and S. Zitrin, *Modern Methods and Applications in Analysis of Explosives*, John Wiley & Sons, 1996.
- 15 J. P. Agrawal and R. Hodgson, *Organic Chemistry of Explosives*, John Wiley & Sons, 2007.
- 16 B. Vogelsanger, *Chim. Int. J. Chem.*, 2004, **58**, 401–408.
- 17 M. Joshi, Y. Delgado, P. Guerra, H. Lai and J. R. Almirall, *Forensic Sci. Int.*, 2009, **188**, 112–118.
- 18 A. H. Lawrence and P. Neudorfl, *Anal. Chem.*, 1988, **60**, 104–109.
- 19 S. Armenta, M. Alcala and M. Blanco, *Anal. Chim. Acta*, 2011, **703**, 114–123.
- 20 G. A. E. Karpas and Z. Karpas, *Ion Mobility Spectrometry, Second Edition*, CRC Press, 2005.

Journal Name

- 1 21 R. G. Ewing, D. A. Atkinson, G. A. Eiceman and G. J. Ewing,
2 *Talanta*, 2001, **54**, 515–529.
- 3 22 G. A. Buttigieg, A. K. Knight, S. Denson, C. Pommier and M.
4 Bonner Denton, *Forensic Sci. Int.*, 2003, **135**, 53–59.
- 5 23 S. Me and M. Cy, *J. Forensic Sci.*, 2001, **46**, 6–11.
- 6 24 E. Sisco, J. Dake and C. Bridge, *Forensic Sci. Int.*, 2013, **232**, 160–
7 168.
- 8 25 A. Stambouli, A. El Bouri, T. Bouayoun and M. A. Bellimam,
9 *Forensic Sci. Int.*, 2004, **146**, S191–S194.
- 10 26 A. Halasz, C. Groom, E. Zhou, L. Paquet, C. Beaulieu, S.
11 Deschamps, A. Corriveau, S. Thiboutot, G. Ampleman, C. Dubois
12 and J. Hawari, *J. Chromatogr. A*, 2002, **963**, 411–418.
- 13 27 S. P. Sharma and S. C. Lahiri, *J. Energ. Mater.*, 2005, **23**, 239–264.
- 14 28 J. Yinon and D.-G. Hwang, *J. Chromatogr. A*, 1983, **268**, 45–53.
- 15 29 B. Casetta and F. Garofolo, *Org. Mass Spectrom.*, 1994, **29**, 517–525.
- 16 30 D. Perret, S. Marchese, A. Gentili, R. Curini, A. Terracciano, E.
17 Bafille and F. Romolo, *Chromatographia*, 2008, **68**, 517–524.
- 18 31 C. N. McEwen, R. G. McKay and B. S. Larsen, *Anal. Chem.*, 2005,
19 **77**, 7826–7831.
- 20 32 G. A. Harris, A. S. Galhena and F. M. Fernandez, *Anal. Chem.*, 2011,
21 **83**, 4508 – 4538.
- 22 33 M. E. Monge, G. A. Harris, P. Dwivedi and F. M. Fernández, *Chem.*
23 *Rev.*, 2013, **113**, 2269–2308.
- 24 34 M. Morelato, A. Beavis, P. Kirkbride and C. Roux, *Forensic Sci. Int.*,
25 2013, **226**, 10–21.
- 26 35 Z. Takats, *Science*, 2004, **306**, 471–473.
- 27 36 M. Zhao, S. Zhang, C. Yang, Y. Xu, Y. Wen, L. Sun and X. Zhang,
28 *J. Forensic Sci.*, 2008, **53**, 807–811.
- 29 37 I. Cotte-Rodríguez, H. Chen and R. G. Cooks, *Chem. Commun.*,
30 2006, 953.
- 31 38 I. Cotte-Rodríguez, H. Hernández-Soto, H. Chen and R. G. Cooks,
32 *Anal. Chem.*, 2008, **80**, 1512–1519.
- 33 39 J. F. Garcia-Reyes, J. D. Harper, G. A. Salazar, N. A. Charipar, Z.
34 Ouyang and R. G. Cooks, *Anal Chem*, 2010, **83**, 1084–1092.
- 35 40 N. Na, C. Zhang, M. Zhao, S. Zhang, C. Yang and X. Fang, *J Mass*
36 *Spectrom*, 2007, **42**, 1079 – 1085.
- 37 41 J. D. Harper, N. A. Charipar, C. C. Mulligan, X. Zhang, R. G. Cooks
38 and Z. Ouyang, *Anal Chem*, 2008, **80**, 9097–9104.
- 39 42 T. P. Forbes, T. M. Brewer and G. Gillen, *Analyst*, 2013, **138**, 5665–
40 5673.
- 41 43 T. P. Forbes and E. Sisco, *Analyst*, 2014, **139**, 2982–2985.
- 42 44 T. P. Forbes and E. Sisco, *Anal. Chem.*, 2014, **86**, 7788–7797.
- 43 45 L. Song, A. B. Dykstra, H. Yao and J. E. Bartmess, *J. Am. Soc. Mass*
44 *Spectrom.*, 2009, **20**, 42–50.
- 45 46 G. A. Harris, L. Nyadong and F. M. Fernandez, *The Analyst*, 2008,
46 **133**, 1297.
- 47 47 D. R. Ifa, A. U. Jackson, G. Paglia and R. G. Cooks, *Anal. Bioanal.*
48 *Chem.*, 2009, **394**, 1995–2008.
- 49 48 J. M. Nilles, T. R. Connell, S. T. Stokes and H. Dupont Durst,
50 *Propellants Explos. Pyrotech.*, 2010, **35**, 446–451.
- 51 49 A. M. Pfaff and R. R. Steiner, *Forensic Sci. Int.*, 2011, **206**, 62–70.
- 52 50 J. H. Gross, *Anal. Bioanal. Chem.*, 2014, **406**, 63–80.
- 53 51 C. N. McEwen and B. S. Larsen, *J. Am. Soc. Mass Spectrom.*, 2009,
54 **20**, 1518–1521.
- 55 52 T. P. Forbes and E. Sisco, *Unpubl. Work*, 2014.
- 56 53 X. Zhao and J. Yinon, *J. Chromatogr. A*, 2002, **977**, 59–68.